JJMIE

Volume 15, Number 1, March. 2021
ISSN 1995-6665
Pages 65 - 71

Jordan Journal of Mechanical and Industrial Engineering

Calculation Method of Stiffness and Deflection of Corroded RC Beam Strengthened by Steel Plate

Qian Zhang[1], Huang Tang[2*], Shihui Guo[3]

[1] Civil Contruction Office, Nanyang Institute of Technology, Nanyang 473000, China
[2] School of Civil Engineering, Hunan City University, Yiyang 413000, China
[3] School of Civil Engineering, Nanyang Institute of Technology, Nanyang 473000, China

Received July 18 2020 Accepted Feb 20 2021

Abstract

Given that corrosion is not considered in calculating the stiffness of reinforced concrete structures under existing cord, this paper improves the calculation formula in cord, and proposes a method to calculate the stiffness of the corroded beam strengthened by steel plate, then the formula for calculating the deflection is proposed. Nine corroded beams are strengthened by steel plates, the static test results of which are used to verify the correctness of calculation method. The influence of corrosion rate and thickness of steel plate on the stiffness are analyzed through the deflection change. Both experimental and theoretical analysis results show that the corrosion rate has a limited impact on the reduction of stiffness. When the thickness of steel plate reaches 6 mm and the corrosion rate reaches 30%, the change in deflection will decrease. At the same time, the influence of corrosion rate on the stiffness is greater than that of steel plate thickness.

Keywords: Steel Plate, Corroded RC Beam, Strengthening, Stiffness, Deflection, Calculation Method.;

1. Introduction

Corrosion of steel bars caused by chloride ion erosion in concrete is the most important reason of structural performance degradation. Over the past few decades, scholars have focused on the structural performance of corroded RC beams. Zhang et al. [1] and Zhang [2] et al. proposed the calculation formula of the ultimate bearing capacity of corroded RC beams, and verified the correctness of models through a series of tests on corroded beams. Sun at al. [3], Maaddawy et al. [4] and Yang [5] et al. have also established models of stiffness degradation model caused by the degeneration of bond stress between corroded steel bar and concrete. Wu [6] et al. studied the deformation performance and failure model of corroded RC beam under fatigue loading. Li [7] and Vidal [8] et al. examined the relationship between corrosion rate and crack width and proposed a calculation model of crack with. Du [9] et al. and Malumbela [10-13] et al. studied the mechanical properties of bending stiffness, stress strain and residual bearing capacity of corroded beams under the stress state.

The strengthening technology of steel plate has been widely used in engineering because of its simple construction, low cost and good strengthening effect. Scholars mainly focuses on the structural behavior of non-corroded beam. Ren et al. [14] studied the influence of anchorage spacing and loading on the strengthening effect of concrete beams strengthened by bonded steel plates. Gao et al. [15] analyzed the influence of amount and position of bonded steel and the width-to-thickness ratio of steel plate on the deformation and bearing capacity of RC beam through test. Raoof [16] et al. proposed the failure model of steel plate and pointed out that the spacing of cracks is the main reason for failure. Altin [17] et al. proposed a method for improving the shear resistance of T-beams strengthened by different side-mounted steel plates. Experiment results show that different shapes and layouts of side-laying modes have different effects on the failure mode and shear capacity of T-beams. Su [18-20] et al. studied the nonlinear behavior of RC beams laterally anchored by steel plate, as well as the influence of anchor placement, and the shear transfer between steel plates and anchors.

The above-mentioned studies on corroded RC beams have not considered the strengthening measures after degradation of mechanical properties. The researches on the strengthened beam also have not considered the corrosion of steel bar. However, in practice, the strengthening strategy is often carried out after the properties of RC structure appears degraded caused by steel bar corrosion. There are few theoretical studies that focused on the deflection behavior of corroded RC beam strengthened by steel plate [21-23].

In this paper, the formulas for calculating the stiffness of RC beams are improved, the stiffness calculation formula of corroded beams strengthened by steel plates is deduced considering the geometric, physical and mechanical equilibrium. Nine corroded beams are strengthened by steel plates, the static test results of which are used to verify the correctness of calculation method. The influence of corrosion rate and thickness of steel plate on the stiffness are analyzed through the deflection change.

* Corresponding author e-mail: guoguo91@126.com.

2. Theoretical Calculation of Stiffness of Corroded Beams Strengthened by Steel Plates

2.1. Analysis of Corrosion Model

The pitting corrosion is more consistent with the actual corrosion pattern of steel bar. Therefore, the pitting corrosion model should be adopted in the calculation model. The model of corroded steel bar proposed by Val [24] is used in this paper, as shown in the follows:

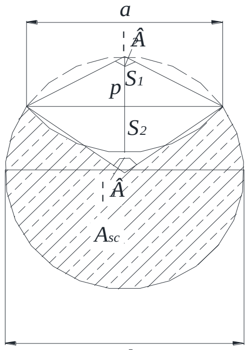

Figure 1. Model of steel bar with pitting corrosion.

The remaining cross-sectional area of steel bar in the model can be expressed as:

$$A_{sc}=\begin{cases}\dfrac{\pi d^2}{4}-S_1-S_2 & p\le\dfrac{\sqrt{2}}{2}d\\ S_1-S_2 & \dfrac{\sqrt{2}}{2}d<p\le d\\ 0 & p>d\end{cases} \tag{1}$$

In the above formula, S_1 and S_2 represent two semi-elliptical areas outside the shaded area, expressed as follows:

$$\begin{aligned}&S_1=\frac{1}{2}\left[\beta_1\left(\frac{d}{2}\right)^2-a\left|\frac{d}{2}-\frac{p^2}{d}\right|\right]\\&A_2=\frac{1}{2}\left[\beta_2 p^2-a\frac{p^2}{d}\right]\\&a=2p\sqrt{1-\left[\frac{p}{d}\right]^2}\\&\beta_1=2\arcsin\left(\frac{2a}{d}\right);\beta_2=2\arcsin\left[\frac{a}{p(t)}\right]\end{aligned} \tag{2}$$

In reference [25], it is pointed out that the yield strength of steel bar with pitting erosion is linear:

$$f_{yc}=(1-\lambda\frac{A_s-A_{sc}}{A_s}\times 100)f_y \tag{3}$$

where f_{yc} is yield strength of steel bar with pitting corrosion, f_y is yield strength of steel bar without corrosion, A_s is cross-sectional area of steel bar without corrosion, λ is the experimental parameter. Through a large number of experiments results for plain steel bars and ribbed steel bars, Peng et al. [26] showed the value of λ is 0.0035.

2.2. Stiffness Analysis of Corroded Steel Bars

To analyze the stiffness of corroded RC beams strengthened by steel plates, the basic assumptions are:

1. The plane cross-section assumption is still applied to concrete strain;
2. Due to the influence of steel bar corrosion, the strain of tensile reinforcement is not compatible with the concrete strain at the same position, and the plane cross-section assumption is no longer applicable;
3. The tensile strength of concrete in the tension zone is no longer considered due to corrosion expansion.

The force of concrete beam strengthened by the steel plate is shown in Fig. 2:

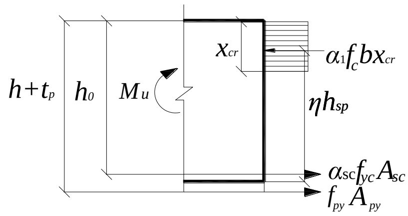

Figure 2. Forced section of the test beam after steel plate reinforcement.

It can be concluded from the equilibrium condition that:

$$\beta(\alpha_{sc}f_{yc}A_{sc}+f_{py}A_{py})=\alpha_1 f_c b x_{cr} \tag{4}$$

$$x_{cr}=\frac{\beta(\alpha_{sc}f_{yc}A_{sc}+f_{py}A_{py})}{b\alpha_1 f_c} \tag{5}$$

where α_{sc} is strength utilization factor of steel bar [1], b is depth of beam, β is coordinated working coefficient of steel plate and longitudinal steel bar, x_{cr} is depth of compressive zone, α_1 is the ratio of the stress value of equivalent rectangle stress diagram to the axial compressive strength, which is obtained according to the Code for Design of Concrete Structures (GB50010-2012).

Assuming that the h_{sp} is the distance from the joint action point of corroded tensile reinforcement and steel plate to the top of e beam, which is obtained from the centroid method [15] that:

$$h_{sp}=\frac{\alpha_{sc}f_{yc}A_{sc}(h-a_s)+f_{py}A_{py}(h+t_p/2)}{\alpha_{sc}f_{yc}A_{sc}+f_{py}A_{py}} \tag{6}$$

The key to calculating the deflection of an RC beam is to find its curvature and stiffness. The experimental results show that the failure process of corroded RC beams strengthened by steel plates is similar to that of corroded RC beams without strengthening. Due to the degradation of bond stress after corrosion, the strain of steel bar in the middle section lags that of concrete. Thus, the incompatibility between steel bar and concrete should be considered.

The stiffness and curvature of the section can be expressed as:

$$B=\frac{M}{\phi} \tag{7}$$

Where, B is flexural stiffness, M is external bending moment, φ is sectional curvature.

According to the stiffness theory in material mechanics, the sectional curvature can be deduced from the geometrical, physical, and equilibrium conditions of the section. Fig. 3 shows the stress distribution of simple bending section and mid-span section of corroded-strengthened beam:

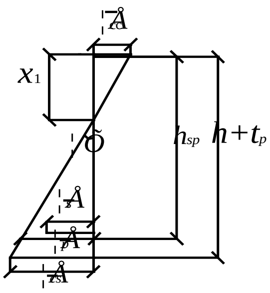

(1)

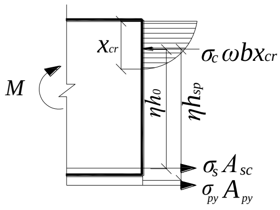

(2)

Figure 3. Stress distribution of simple bending section and mid-span section.

(1) Geometrical condition:

$$\phi=\frac{p(\eta_s)q(\eta_s)\cdot\psi\cdot\varepsilon_s+\varepsilon_{cc}+\varepsilon_p}{h_{sp}} \tag{8}$$

where ε_{cc} is concrete strain at the top of compression zone, ε_s is concrete strain near the tensile steel bar, ε_p is the average strain of bottom steel plate, h_{sp} is effective height of converted section, $p(\eta_s)$ is strain incompatibility coefficient of steel bars [27], $q(\eta_s)$ is cohesion degradation correction factor, ψ is obtained according to the Code for Design of Concrete Structures (GB50010—2012).

(2) Physical relationship between stress and strain

The stress distribution of crack section is shown in Fig. 3. The stress-strain relationship of the top concrete, tensile reinforcement and steel plate is expressed as:

$$\varepsilon_{cc}=\frac{\sigma_c}{E_c},\quad \varepsilon_s=\frac{\sigma_s}{E_s},\quad \varepsilon_p=\frac{\sigma_{py}}{E_p} \tag{9}$$

where, σ_c is concrete stress on top of beam, σ_s is stress of tensile steel bar, σ_{py} is steel plate stress, E_c is elasticity modulus of concrete, E_s is elasticity modulus of tensile steel bar, E_P is elasticity modulus of steel plate.

(3) Equilibrium condition of stress

Based on the stress distribution in Fig.s (2) and (3), the equilibrium equation can be obtained:

$$M=\omega\sigma_c b x_{cr}\eta h_{sp} \tag{10-a}$$

$$M=\omega\sigma_c b x_{cr}\eta h_0+\sigma_{py}A_{py}(a_s+\frac{d}{2}+\frac{t_p}{2}) \tag{10-b}$$

$$\omega\sigma_c b x_{cr}=\sigma_s A_{sc}+\sigma_{py}A_{py} \tag{10-c}$$

where M is the bending moment of cross section, ω is the stress and shape integrity coefficient in the compressed zone, η is the coefficient of internal force arm on crack section, h_0 is the effective height of section.

Combining the above three conditions in formula (7) and (8), we conclude that the short-term stiffness of corroded-strengthened beam is:

$$B=\frac{E_s A_{py} h_{sp}^2}{p(\eta_s)q(\eta_s)\psi A_{py}\frac{2a_s+d+t_p-2\eta\left(h_{sp}-h_0\right)}{\eta(2a_s+d+t_p)A_{sc}}+\alpha_s\frac{A_{py}}{\omega b x_{cr}\eta}+\frac{2\alpha_s\left(h_{sp}-h_0\right)}{a_s+d+t_p}} \tag{11}$$

After the bending stiffness is obtained, the following simplified formula can be used to calculate the deflection value of beam [15]:

$$\delta=S\frac{Ml_0^2}{B} \tag{12}$$

where S denotes the deflection calculation coefficient related to the load and the support condition, S is 13/216 for 4-point loading and S is 1/12 for mid-span concentrated load.

3. Experimental Investigation

3.1. Design of Tested Beam

There is a total of 9 tested beams. The reinforcement details of the specimens are shown in Fig. 4. Each specimen is 1,800 mm long, 150 mm wide, and 300 mm deep with a rectangular cross section and reinforced by two 22-mm-diameter (hot-rolled ribbed reinforcement steel bars) bottom longitudinal deformed reinforcing bars, two 16-mm-diameter top longitudinal deformed reinforcing bars, and 8-mm-diameter epoxy-coated deformed reinforcing stirrups spaced at 100 mm at the middle and 70 mm at the ends. A typical clear cover of 30 mm was used all around the stirrups.

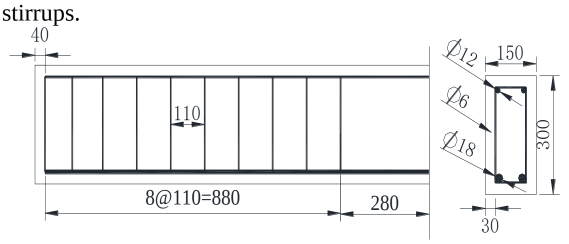

Figure 4. Test beam reinforcement drawing.

3.2. Test Material Properties

The average compressive strength of concrete measured by concrete strength test is 29.85 MPa. The yield strength of stirrups, compression and tensile reinforcement is respectively 338 MPa, 336 MPa and 340 MPa. All steel bars have a modulus of elasticity of 200 GPa. The yield strength of the reinforced steel plate is 238 MPa. The adhesive layer uses JN-S structural adhesive produced by Good Bond Company. The layer boasts a compressive strength of 89.5 MPa and a bonding strength with concrete of 4.0 MPa.

3.3. Corrosion of Tensile Steel bar and Installation of Steel Plate

As shown in Fig. 5, beams are immersed horizontally in a steel iron water tank, which has a size of 2,200 mm long, 700 mm wide, and 800 mm high, to a depth of about 200 mm in a 5% NaCl solution. Both ends of all specimens are placed above the concrete blocks and immersed up to one-third of their height in the solution. Distilled water is used to prepare the solution. A stainless-steel plate of 1.2 ×350 × 1,800 mm is immersed in the solution to be used as a counter electrode. The positive output is connected to the deformed bar, whereas the negative output is connected to the stainless-steel plate. The current supplied to each specimen is checked on a regular schedule and any shift is corrected by adjusting the ammeter, which monitored the cell current. The current intensity of the power supply and the corrosion period are selected for each beam in order to achieve the desired degree of corrosion of the submerged reinforcing bar. Therefore, a constant current of 1,760 mA was applied to each specimen for a period of 12 days to obtain theoretical mass loss of 10% in tension. The corrosion rate of 9 tested beams was divided into 3 grades, respectively of 10%, 20% and 30%. The thickness of steel plate is divided into 3 levels, 2 mm, 4 mm and 6 mm. The steel corrosion and steel plate layout are shown in Fig. 5 (1) and (2).

(1) Fast electrochemical corrosion

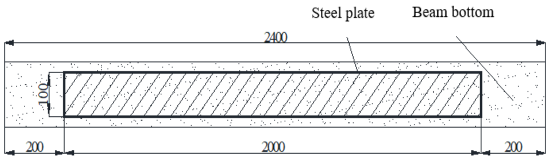

(2) Schematic diagram of bonded steel plate

Figure 5. Steel corrosion and bonded steel plate.

3.4. Loading Method

Following the corrosion period and strengthening work, all specimens were monotonically loaded in midpoint loading (Fig. 6). The load is applied using a 500 kN hydraulic jack through a bearing plate to the beam specimens. Per loading increment is 5 kN at the beginning of loading. The strain and deflection of steel plate across the middle and 1/4 span were recorded. The distribution of cracks on both sides of tested beam is also depicted.

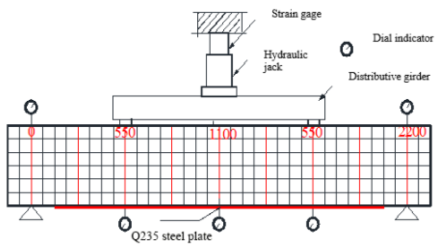

Figure 6. Test beam loading

4. Discussion of Tested Results

4.1. Corrosion of steel bar

Fig. 7 presents corrosion-induced cracks distribution of the beam specimens P1 and P2. It can be observed from Fig. 7 that the longitudinal corrosion-induced cracks are mainly on the side face along the longitudinal main reinforcements of beam specimens. This is resulted from the radial stress induced by the corrosion products exceeding concrete tensile strength. However, there is difference for the corrosion-induced crack distribution of each beam because of the non-uniform pitting corrosion. The factors such as impressed current density, the PH of NaCl solution and penetration rate of the Cl^- ions varies in the process of corrosion, which leads to the dispersion of corrosion pit on the surface of the steel bar, and then the corrosion-induced cracks distribution will be different. The corrosion conditions of tensile bars that are respectively located at 10 cm to 40 cm of beam specimen P1 and 40 cm to 80 cm of beam specimen P2 are also shown in Fig. 8. As can be observed in Fig. 7, the corrosion of tensile steel reinforcements has already reached the generalized corrosion stage defined by Zhang et al. [28]. In this stage, there is corrosion all along the bars, and there are also some zones where pit corrosion is significant.

4.1.1. Influence of steel plate thickness on the deformation of beam

Because there is a deviation between the measured corrosion rate and the design value in this test, beams with the similar corrosion rate are selected for comparison. Fig. 7 is the load-mid-span deflection curve of the test beam with the same protective layer and different thickness of steel plate. As can be seen from Fig.8, when the thickness of concrete protective layer is the same and the corrosion rate of steel bar is similar, the stiffness of the test beam is obviously lager as the thickness of steel plate increases from 2 to 4 mm. However, as the thickness of steel plate continues to increase, the steel degree of the test beam increases gradually. Under the same load, the mid-span deflection of the strengthened beam decreases with the increase of the reinforcement thickness of steel plate. The ductility of the stiffness of test beam decreases with the increase of the thickness of steel plate.

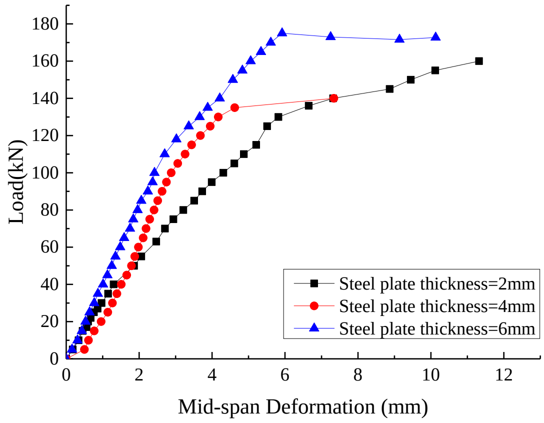

Figure 8. Load-mid-span deflection of beam with cover thickness=35mm

4.2. Influence of the thickness of protective layer on the deformation performance of the beam

Fig. 9 shows the load-mid-span deflection curve of test beam with different thickness of concrete cover with the same thickness of steel plate. As shown in Fig. 8, when the thickness of steel plate is 4 mm, the thickness of the concrete protective layer is changed, and the P–δ curves of each test beam are very close in the loading process. This indicates that when the corrosion rate of reinforcement is similar, the thickness of steel plate is the same when the corroded beam is strengthened, and the deformation performance of the beam is less affected by changing the thickness of the concrete protective layer.

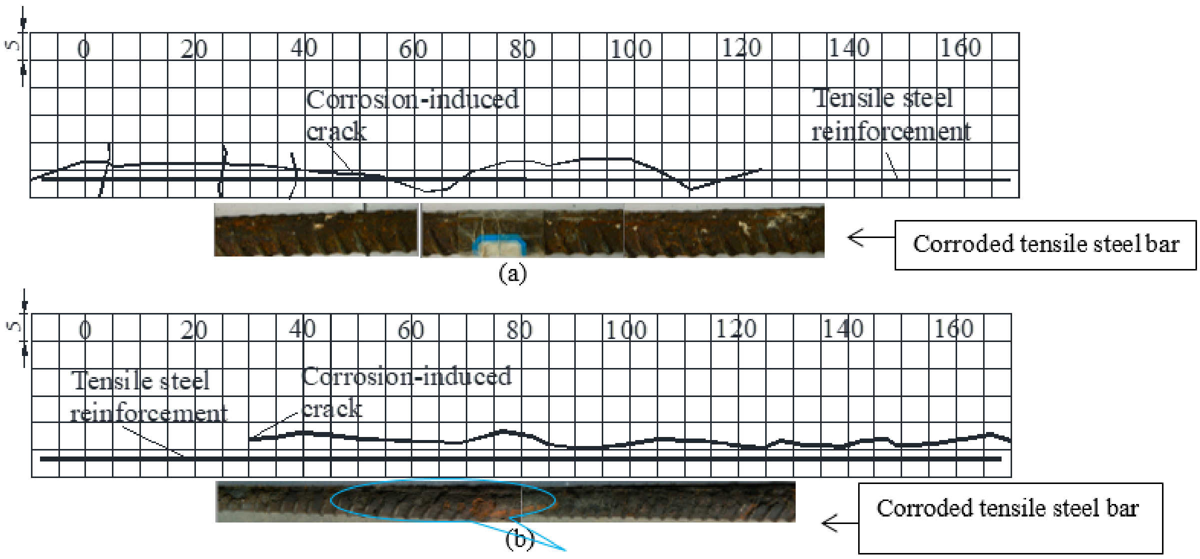

Figure 7. Corrosion-induced cracks distribution of the beam specimens and corrosion condition of tensile steel reinforcement: (a) P1; (b) P2

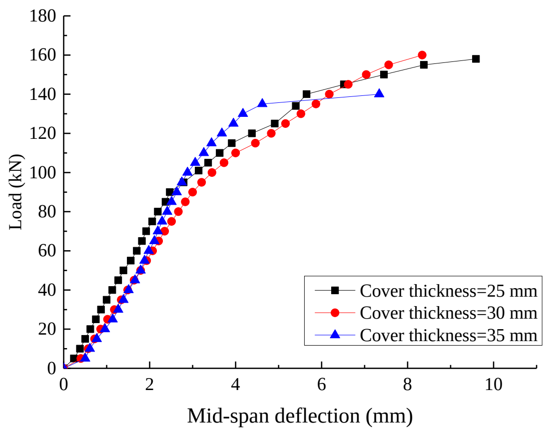

Figure 9. Load-mid-span deflection of beam with steel plate thickness=4mm

4.3. Comparison of Tested Values with Theoretical Values of Deflection

A comparison of theoretical and experimental values of mid-span ultimate deflection is given in Table 1, which shows that the theoretical value of ultimate deflection is close to the experimental value. The correlation between the tested value and theoretical value is listed in Fig. 10. The ratio of tested value to theoretical value ranges from 1.01 to 1.11, and the mean and coefficient of ratio variation are respectively 1.04 and 0.037. The results show that the theoretical formulas of stiffness and deflection presented in this paper can be used to predict the tested values.

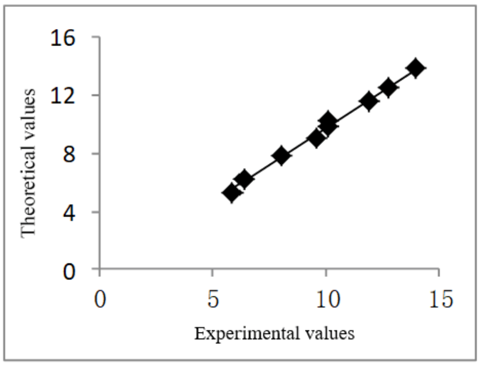

Figure 10. Correlation between theoretical values and tested values.

Theoretical and tested results show that when the steel plate increased by 2 mm and the corrosion rate is close, For example, beams P1 and P2, beams P4 and P5, the ultimate mid-span deflection of decreased by about 2.7 mm. Comparing beams P7, P8 and P9, it can be found that when the corrosion rate reaches about 30%, the mid-span deflection decreases as stiffness increases. It shows that the influence of thickness of steel plate on the increase of stiffness is not linearly. When the thickness of steel plate exceeds a certain value, the ultimate bearing capacity and stiffness no longer increase linearly [15, 29, 30].

Under the condition of same thickness of steel plate, when the corrosion rate is less than 20%, the deflection increases about 3 mm as the corrosion rate is increased by 10%. This shows that the influence of corrosion rate on the deflection of corroded-strengthened beams is greater than the thickness of the steel plate. When the corrosion rate reaches 30%, the increased deflection of beam compared with beam with 20% corrosion rate is lower than that between beams with 10% and 20% corrosion rate It is also stated that the corrosion rate has a limited effect on the reduction in stiffness.

Table 1. Comparison of calculated and tested values of deflection theory.

No.	*t* (mm)	*c* (mm)	f_c (MPa)	Average corrosion rate	δ (mm) theoretical value	δ (mm) experimental value
P1	2	25	30.4	9.60%	9.56	9.06
P 2	4	25	29.8	11.20%	6.38	6.28
P 3	6	25	29.5	11.60%	5.89	5.3
P 4	2	30	30.6	19.80%	12.8	12.5
P 5	4	30	29.9	20.50%	10.1	9.8
P 6	6	30	30	21.50%	8.03	7.8
P 7	2	35	28.5	31.5%	13.97	13.84
P 8	4	35	29.6	28.91%	11.95	11.60
P 9	6	35	30.4	29.8%	10.1	10.21

5. CONCLUSIONS

This paper revises the formula in cord and proposes the formula for calculating the stiffness and deflection of corroded beams strengthened by steel plate. The correctness of deflection formula is verified by the test study of nine corroded-strengthened beams. At the same time, the influence of the thickness of steel plate and corrosion rate on the stiffness of corroded-strengthened beam is analyzed. following conclusions can be drawn:

1. The theoretical results of mid-span deflection are close to the tested results. The theoretical calculation formula can better predict the stiffness and deflection values of corroded beams strengthened by steel plate.
2. The corrosion rate has a limited influence on the reduction of stiffness. When the thickness of steel plate reaches 6 mm and the corrosion rate reaches 30%, the change of deflection will decrease.
3. When the thickness of steel plate exceeds a certain value, the ultimate bearing capacity and stiffness no longer increase linearly.
4. Comparing the influence of both the thickness of the steel plate and corrosion rate on the deflection, it can be found that the effect of the corrosion rate on the stiffness is greater than that of steel plate thickness.

Acknowledgment

This work was supported by Fund Program: Henan provincial science and technology key project-international cooperation (182102410068), Natural Science Foundation of Hunan Province (Grants nos. 2019JJ50023), 2020 Yincheng Science and Technology Talents Supporting Project of Yiyang.

References

[1] Zhang, X., Wang, L., Zhang, J. and Liu, Y., **2016**. Model for flexural strength calculation of corroded RC beams considering bond–slip behavior. *Journal of Engineering Mechanics*, *142*(7): 04016038.

[2] Zhang, J.R., Zhang, K.B., Peng, H. and Gui, C., **2009**. Calculation method of normal section flexural capacity of corroded reinforced concrete rectangular beams. *China Journal of Highway and Transport*, *22*(3), pp.45-51.

[3] Sun, B., Niu, D.T. and Wang, Q.L., **2004**. Analysis and calculation of bending stiffness of corroded reinforced concrete beams. *Building Structure*, *10*, pp.42-45.

[4] Maaddawy, T.E., Soudki, K. and Topper, T., **2005**. Analytical model to predict nonlinear flexural behavior of corroded reinforced concrete beams. *ACI Structural Journal 102*(4), pp.550-559.

[5] Yang, S.Y., Liu, X.L. and Leng, Y.B., **2012**. Prediction of flexural deformation of a corroded RC beam with a polynomial tension-stiffening model. *Journal of Structural Engineering*, *139*(6), pp.940-948

[6] Wu, J., Wang, C.X., Xu, J., Xiao, Z. and Wu, F.H., **2012**. Study on flexural behavior of corroded reinforced concrete beams under fatigue loads. *China Civil Engineering Journal*, *10*, pp.118-124.

[7] Brandonisio, G., Lucibello, G., Mele, E. and Luca, A.D., **2013**. Damage and performance evaluation of masonry churches in the 2009 L'Aquila earthquake. *Engineering Failure Analysis*, *34*(0), pp.693-714.

[8] Harish, K.V., Dattatreya, J.K. and Neelamegam, M., **2013**. Experimental investigation and analytical modeling of the σ–ε characteristics in compression of heat-treated ultra-high strength mortars produced from conventional materials. *Construction and Building Materials*, *49*(0), pp.781-796.

[9] Du, Y.G., Cullen, M. and Li, C., **2012**. Structural performance of RC beams under simultaneous loading and reinforcement corrosion. *Construction and Building Materials*, *38*, pp.472-481.

[10] Malumbela, G., Alexander, M., and Moyo, P., **2009**. Steel corrosion on RC structures under sustained service loads-A critical review. *Engineering Structures*, *31*(11), pp.2518-2525.

[11] Malumbela, G., Alexander, M. and Moyo, P., **2010**. Lateral deformation of RC beams under simultaneous load and steel corrosion. *Construction and Building Materials*, *24*(1), pp.17-24.

[12] Malumbela, G., Alexander, M. and Moyo, P., **2010**. Variation of steel loss and its effect on the ultimate flexural capacity of RC beams corroded and repaired under load. *Construction and Building Materials*, *24*(6), pp.1051-1059.

[13] Malumbela, G., Moyo, P. and Alexander, M., **2012**. Longitudinal strains and stiffness of RC Beams under load as measures of corrosion levels. *Engineering Structures*, *35*, pp.215-227.

[14] Ren, W., He, S.H., Zhao, X.X. and Luan, H.F., **2008**. Model test on preloaded RC T-beam strengthened by bonded steel plates. *China Journal of Highway and Transport*, *03*, pp.64-68.

[15] Gao, X.N., Zhou, Q.Y. and Chen, M.H., **2006**. Theoretical and experimental research on bearing behavior of RC beams strengthened by bonded steel plates. *China Civil Engineering Journal*, *39*(8), pp.38-44.

[16] Raoof, M., El-Rimawi, J.A. and Hassanen, M.A.H., **2000**. Theoretical and experimental study on externally plated R.C. beams. *Engineering Structures*, *22*(1), pp.85-101.

[17] Altin, S., Anil, Ö. and Kara, M.E., **2005**. Improving shear capacity of existing RC beams using external bonding of steel plates. *Engineering Structures*, *27*(5), pp.781-791.

[18] Siu, W.H. and Su, R.K.L., **2010**. Effects of plastic hinges on partial interaction behaviour of bolted side-plated beams. *Journal of Constructional Steel Research*, *66*(5), pp.622-633.

[19] Su, R.K.L., Li, L.Z. and Lo, S.H. **2013**. Shear transfer in bolted side-plated reinforced concrete beams. *Engineering Structures*, *56*(0), pp.1372-1383.

[20] Su, R.K.L., Siu, W.H. and Smith, S.T., **2010**. Effects of bolt–plate arrangements on steel plate strengthened reinforced concrete beams. *Engineering Structures*, *32*(6), pp.1769-1778.

[21] Jiang, Z. and Jia, Z., **2018**. Effects of students basketball club participation motivation on club cohesion organizational commitment as the mediator. *Journal of Interdisciplinary Mathematics*, *21*(2), pp.519-528.

[22] Chen, D.Z., **2018**. Performance evaluation model for government-supportive urbanization. *Journal of Discrete Mathematical Sciences and Cryptography*, *221*(4), pp.859-868.

[23] Ekman, J., Hietaniemi, M., Kolari, M., Nelson, M. and Keegan, K., **2017**. Novel starch saving programme improves sustainability in board manufacturing through the reuse of recycled fibre starch. *Paper Asia*, *33*(6), pp.18-22.

[24] Val, D.V. and Melchers, R., **1997**. Reliability of deteriorating RC slab bridges. *Journal of Structural Engineering*, *123*(12), pp.1638-1644.

[25] Stewart, M.G., **2009**. Mechanical behaviour of pitting corrosion of flexural and shear reinforcement and its effect on structural reliability of corroding RC beams. *Structural Safety*, *31*(1), pp.19-30.

[26] Peng, J.X., Zhang, J.R., Zhang, K.B. and Peng, H., **2012**. Probabilistic Resistance Model and experimental investigation on for corroded RC bridges. *Engineering Mechanics*, *29*(6), pp.125-131.

[27] Sun, B., **2006**. Structural performance degrading and seismic evaluation of existing reinforced concrete structures. Xi'an: Xi'an University of Architecture and Technology.

[28] Li, J., **2020**. Distributed multi-level inventory algorithms for automotive maintenance spare parts based on centralized control model. *Jordan Journal of Mechanical and Industrial Engineering, 14*(1), 89-99.

[29] Sedelnikov, A.V., Filippov, A.S. and Ivashova, T.A., **2018**. Earth's magnetic field measurements data accuracy evaluation on board of the small spacecraft "AIST" flight model. *Jordan Journal of Mechanical and Industrial Engineering, 12*(4), 253-260.

[30] Zhang, R., Castel, A. and François, R., **2010**. Concrete cover cracking with reinforcement corrosion of RC beam during chloride-induced corrosion process. *Cement and Concrete Research, 40*(3), 415–425.